Electronic Supplementary Material (ESI) for Journal of Materials Chemistry A.
This journal is © The Royal Society of Chemistry 2022

Electronic Supplementary Information for

Drastic Improvement in Photoelectrochemical Water Splitting Performance over Prolonged Reaction Time Using New Carrier-Guiding Semiconductor Nanostructures

Siyun Noh,[a] Jihoon Song,[b] Sangmoon Han,[†a] Jaehyeok Shin,[a] Yeon-Tae Yu,[a] and Jin Soo Kim[*a]

[a]Department of Electronic and Information Materials Engineering, Division of Advanced Materials Engineering, and Research Center of Advanced Materials Development, Jeonbuk National University, Jeonju 54896, South Korea.
[b]Semiconductor Laboratory, Wonik IPS Co., Pyeongtaek 17746, South Korea.
[†]Present address: Mechanical Engineering and Materials Science, Washington University in Saint Louis, MO, 63130, USA.

*Corresponding author: (e-mail) kjinsoo@jbnu.ac.kr; (Tel.) +82-63-270-2291; (Fax) +82-63-270-2305

Experimental methods

Preparation of photocathodes (PCs). The InGaN/GaN core-shell nanowires (CSNWs) with a protruding shape, used as a PC for the photoelectrochemical water splitting (PEC-WS), were formed on Si(111) with a plasma-assisted molecular-beam epitaxy system. The degree of vacuum was maintained at 1.1×10^{-10} Torr at the initial standby state. Before the growth of nanowires (NWs), the substrate was annealed at 900 °C for an hour and N-plasma source with a purity of 99.9999% was suppled at 800 °C for 10 minutes in order to form a SiN_x layer. And then, a Ga flux was only supplied on the surface of SiN_x/Si(111) at the growth temperature of 915 °C for 6 seconds to form Ga droplets, which is *so-called* Ga pre-deposition method.[1-4] The Ga droplets not only serve nucleation sites, but also contribute to the uniform growth for the subsequent NWs. In addition, they can reduce chemical contamination typically happened during the formation of NWs using a vapor-liquid-solid process.[5] After the formation of Ga droplets, Ga and N-plasma fluxes were simultaneously supplied for an hour and a half to form GaN NWs used as nucleation seeds. The detailed growth conditions for GaN NWs has been described in our previous works.[2-4] After the growth of the GaN NWs, In, Ga, and N-plasma fluxes were simultaneously supplied to form InGaN NWs for four hours at the growth temperature of 670 °C. Instead of forming single-material InGaN NWs, InGaN/GaN CSNWs were spontaneously formed on the GaN NWs due to the lattice mismatch between GaN and InGaN and the difference in the migration length between In and Ga adatoms.[6]

Structural and optical characterization. A field-emission scanning-electron microscopy (FE-SEM, installed in the Future Energy Convergence Core Center at Jeonbuk National University) with a model of Hitachi SU-70 and an aberration-corrected transmission-electron microscopy (Cs-TEM) with a model of Jeol Jem-Arm200F equipped with the electron-dispersive spectroscopy were used for the structural characterization. X-ray diffraction (XRD) with a model of Rigaku Max-2500 was also used. X-ray photoelectron spectroscopy (XPS)

measurements were performed using a model of Thermo Fisher Scientific K-Alpha ESCA system with a micro-focused monochromatic Al Kα source. For photoluminescence (PL) measurements, a diode-pumped solid-state laser with the wavelength of 266 nm was used to detect luminescence from the NW samples. A monochromator with a length of 0.5 m was used. A UV-visible spectrophotometer with a model of Shimadzu UV-2550 was used to analyze the absorption properties. The slit size for UV-visible spectrophotometer was set as 5 nm.

PEC-WS measurements. The PEC-WS measurements were carried out using a potentiostat with a model of Garmy Reference-3000 in a three-electrode configuration with the working electrode area about 0.25 cm^2 and the left part covered by non-sticking polytetrafluorethylene. 0.5-M H_2SO_4 was used as electrolyte and its pH value was 0.3. According to the Nernst equation, the measured voltage could be converted into the potential versus reversible hydrogen electrode (RHE).[7] A xenon lamp with a model of McScience MAX-303 was employed as the light source with a power density of 100 mW/cm^2. The current density (J)-voltage (V) characteristic curves were recorded by sweeping the potential from -1 V to 0 V versus RHE. Electrochemical impedance spectra measurements (EIS) were performed by applying -1 V versus RHE at a frequency range of 100 kHz to 0.1 Hz with an amplitude of 10 mV under illumination condition.

Structural and optical characteristics of GaN NWs

The cross-sectional FE-SEM image of the GaN NWs is shown in Fig. S1a, where the inset is the plan-view image. The average height and diameter of the GaN NWs were measured to be 304.6 and 71.3 nm, respectively. Fig. S1b shows an XRD rocking curve of the GaN NWs. The strong peak observed at 28.3° originates from Si(111). The peaks related to GaN(0002) and GaN(0004) are clearly observed at 34.5° and 72.8°, respectively. These results are in good agreement with GaN in the wurtzite structure and Si with the cubic structure.[8] The full width at half maximum (FWHM) of the GaN(0002) peak was measured to be 0.15°, which is much narrower than those (~1.5°) of the previous reports.[9,10] This result indicates that GaN NWs with high crystal quality were successfully formed on Si(111). Fig. S1c shows PL spectrum of GaN NWs measured at room temperature. The free-exciton peak of GaN NWs is clearly observed at the wavelength of 368 nm. In most of the previous works, it is difficult to observe the free-exciton peak from Si-based GaN NWs at room temperature,[11,12] largely because of the significant influence of defects working as trap sites for photo-generated carriers and consequently reducing the radiative recombination rate.[13] This result indicates the formation of highly-crystalline GaN NWs, which is well consistent with the XRD data. Fig. S1d shows a TEM image of a GaN NW. Fig. S1e shows the HR-TEM images and diffraction patterns (inset) for the top, middle, and bottom regions of a GaN NW. Stacking faults and defects, typically observed from III-V semiconductor NWs formed on Si, are rarely observed in all HR-TEM images.

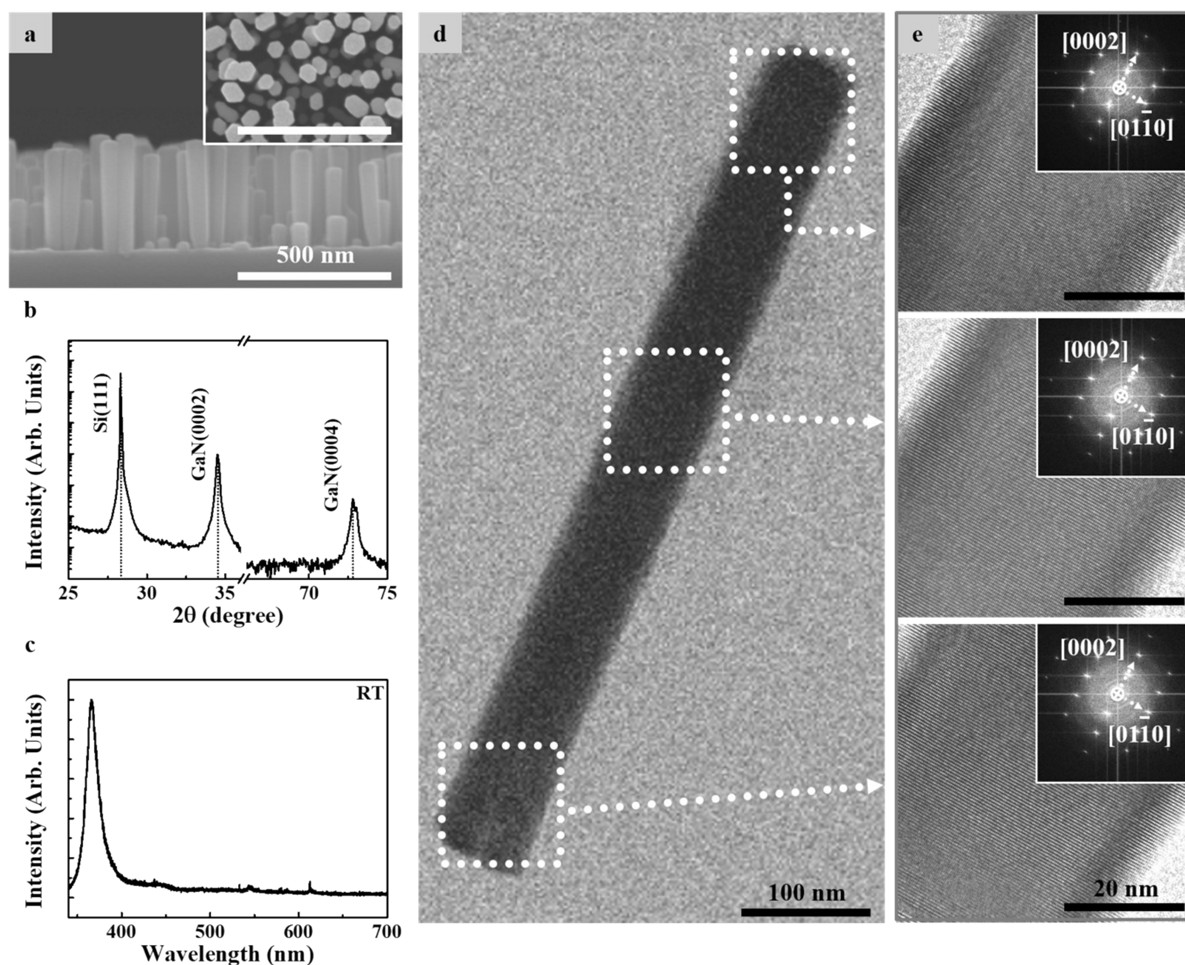

Fig. S1. (a) Cross-sectional FE-SEM image of GaN NWs, where the inset is the plan-view image. (b) XRD rocking curve and (c) PL spectrum of the GaN NWs. (d) TEM image of a GaN NW. (e) HR-TEM images and diffraction patterns (inset) measured at the top, middle, and bottom regions of a GaN NW.

Growth mechanism of InGaN/GaN CSNWs

The InGaN/GaN CSNWs were spontaneously formed on Si(111) as schematically illustrated in Fig. S2. For the formation of the InGaN/GaN CSNW on the GaN NW worked as a nucleation site, there are two components of adatoms; one is directly supplied to the top surface of the GaN NW and the other comes up through the sidewall of the NW. The In, Ga, and N adatoms arriving on the top surface of GaN contribute to forming an InGaN island rather than a disk structure that fully stacked on the bottom GaN surface, mainly due to the relaxation of strain according to elastic energy and surface energy.[14] And then, the InGaN-GaN CSNW structure is spontaneously formed via the island, due to the difference in migration length between In atoms and Ga atoms.

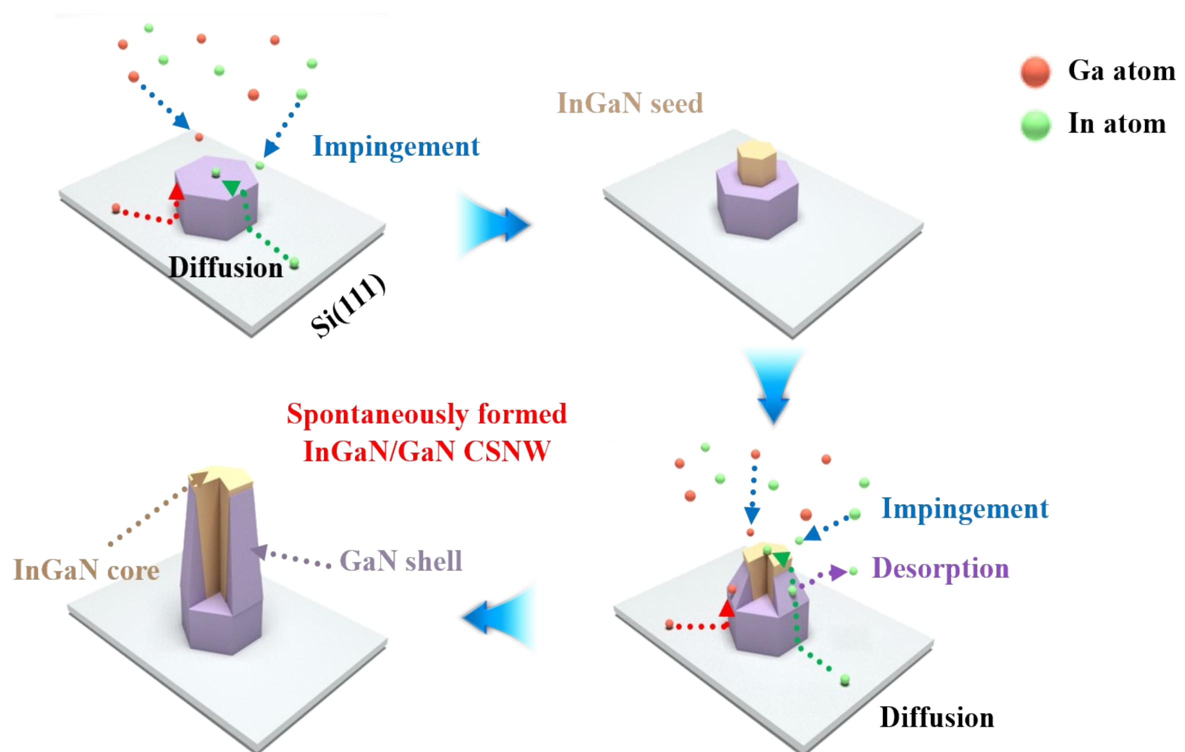

Fig. S2. Schematic illustration for the growth for an InGaN/GaN CSNW.

***J-V* characteristic curves of the GaN-NW PA and InGaN/GaN-CSNW PC measured under dark condition**

Fig. S3 shows the *J-V* characteristic curves of the GaN-NW photoanode (PA) and InGaN/GaN-CSNW PC in the voltage range from -1 to 0 V versus RHE measured under dark condition. The current densities of the GaN-NW PA and the InGaN/GaN-CSNW PC were measured to be 0.12 and 0.21 mA/cm^2, respectively, at -1 V versus RHE.

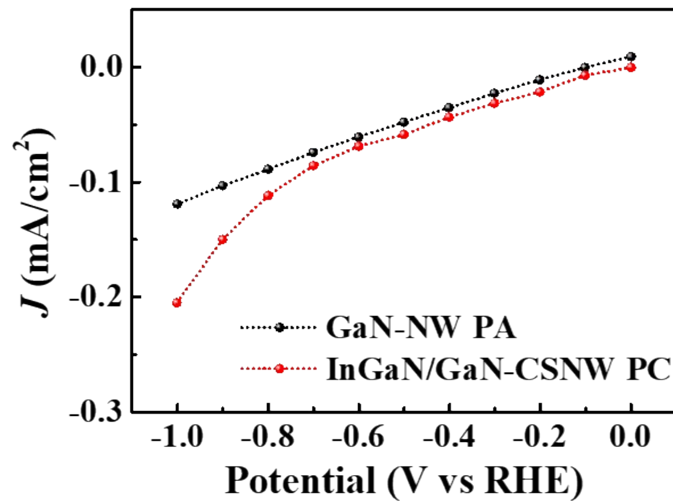

Fig. S3. *J-V* characteristic curves of the GaN-NW PA and the InGaN/GaN-CSNW PC as a function of the potential under dark condition.

Effect of the length of InGaN/GaN CSNWs on the PEC-WS performance

Fig. S4a shows the cross-sectional and plan-view (inset) FE-SEM images of the InGaN/GaN CSNWs with the length of 218±9 (CSNW1), 272±3 (CSNW2), and 378±5 nm (CSNW3). Fig. S4b and c show the current densities and ABPE curves of the CSNW1, CSNW2, and CSNW3 PCs. The current densities (maximum ABPE) of the CSNW1, CSNW2, and CSNW3 PCs were measured to be 6.71 (1.62), 9.95 (2.28), and 28.25 mA/cm^2 (7.07%), respectively, at -1 V versus RHE.

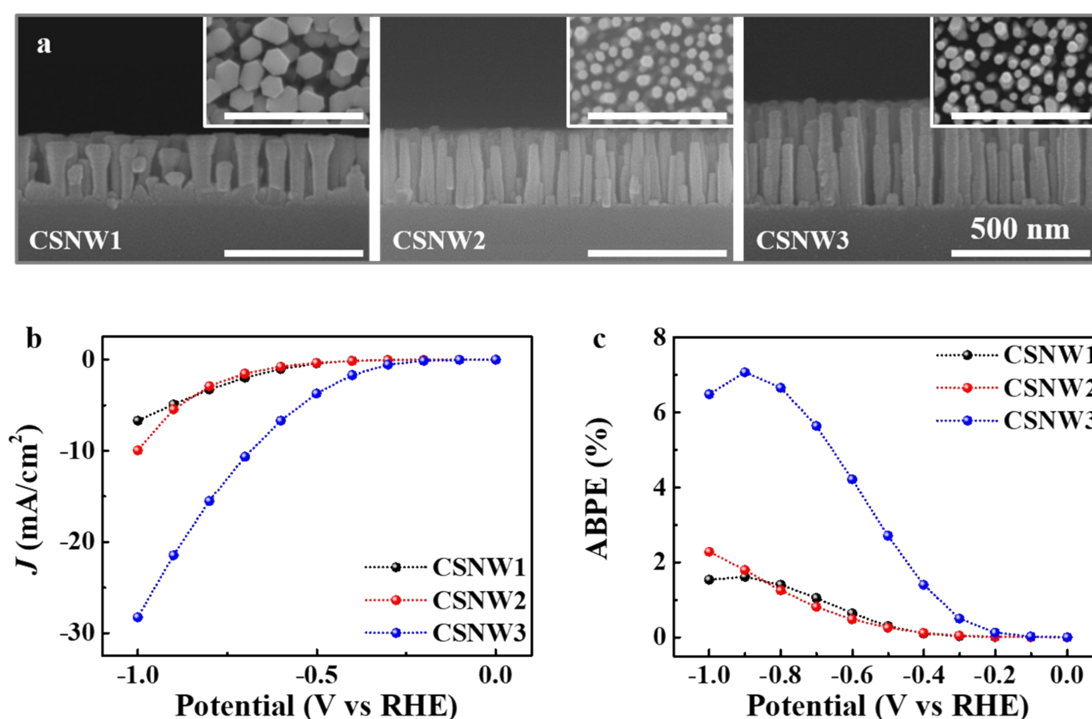

Fig. S4. (a) Cross-sectional and plan-view (inset) FE-SEM images of the CSNW1, CSNW2, and CSNW3 samples. (b) *J-V* characteristic curves and (c) ABPE curves of the CSNW1, CSNW2, and CSNW3 PCs measured under light illumination.

XRD rocking curves of InGaN/GaN-CSNW PC measured before the PEC-WS reaction started and after ten hours of PEC-WS

Fig. S5 shows the original XRD rocking curves of the InGaN/GaN-CSNW PC measured before the PEC-WS started and after ten hours of PEC-WS. For the 2θ-XRD rocking curve measured after ten hours of the PEC-WS reaction, the peaks observed at 34.14^o and 34.50^o are corresponding to InGaN(0002) and GaN (0002), respectively. The FWHMs of the InGaN(0002) and GaN(0002) peaks were measured to be 0.58 and 0.16^o, respectively. The peak positions and their FWHMs are well consistent with those of the initial InGaN/GaN CSNWs.

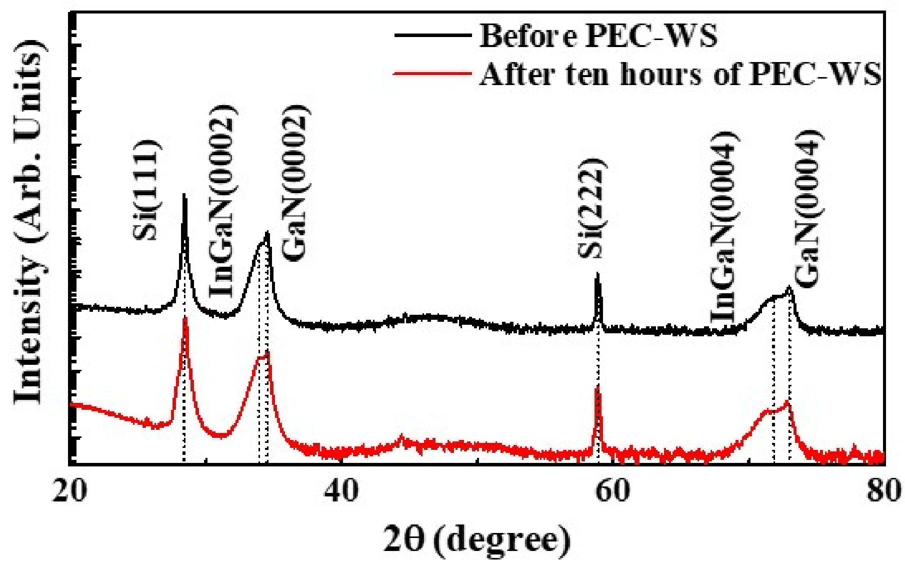

Fig. S5. XRD rocking curves of the InGaN/GaN-CSNW PC.

Electron-dispersive spectroscopy (EDS) line-scan data of the InGaN/GaN CSNWs

Fig. S6 shows EDS line-scan data of a single InGaN/GaN-CSNW PC measured after ten hours of the PEC-WS reaction. The EDS line-scan data was measured along the perpendicular direction to the growth direction at the top and the bottom regions of the InGaN/GaN CSNW. For the top (bottom) region, the diameter of the InGaN core and the thickness of GaN shell were measured to be 26.42 (22.28) and 7.75 nm (12.45 nm), respectively, which are well-matched with those of the InGaN/GaN CSNW measured before the PEC-WS reaction. This result indicates that the structure of the InGaN/GaN-CSNW PC was not affected by the harsh aqueous electrolyte even after long-term PEC-WS reaction.

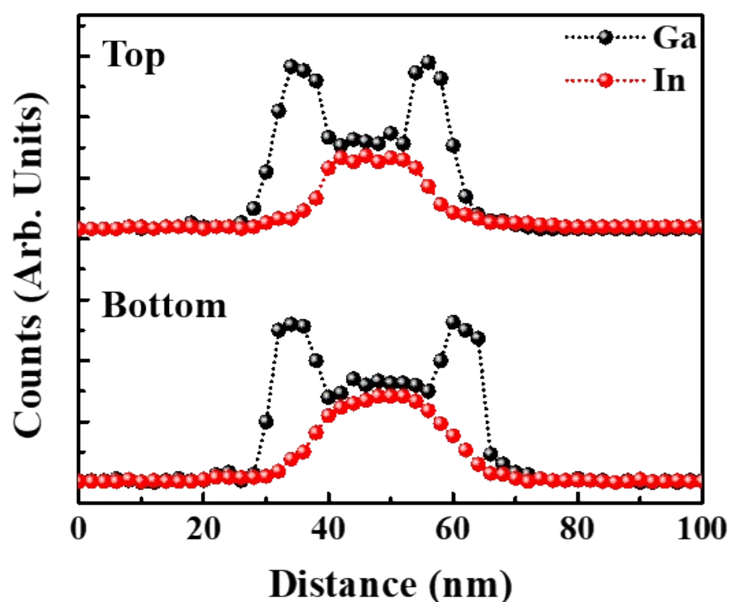

Fig. S6. EDS line-scan data of a single InGaN/GaN-CSNW PC measured after ten hours of the PEC-WS reaction.

XPS data of InGaN/GaN CSNWs

Fig. S7a shows original XPS curves of the InGaN/GaN-CSNW PC measured before PEC-WS and after ten hours of the PEC-WS reaction. Fig. S7b, c, and d show the expanded XPS curves. As shown in Fig. S7b, the binding energies of Ga 3d (20.23 eV), In 4d (19.26 eV), and N 1s (17.79 eV) are consistent with those of the initial InGaN/GaN-CSNWs. In Fig. S7c and d, three peaks were observed at 444.04 (In $4d_{3/2}$), 451.55 (In $4d_{5/2}$), and 397.36 eV (N 1s) after ten hour operation of the InGaN/GaN-CSNW PC, which are same as those obtained at the initial InGaN/GaN CSNWs.

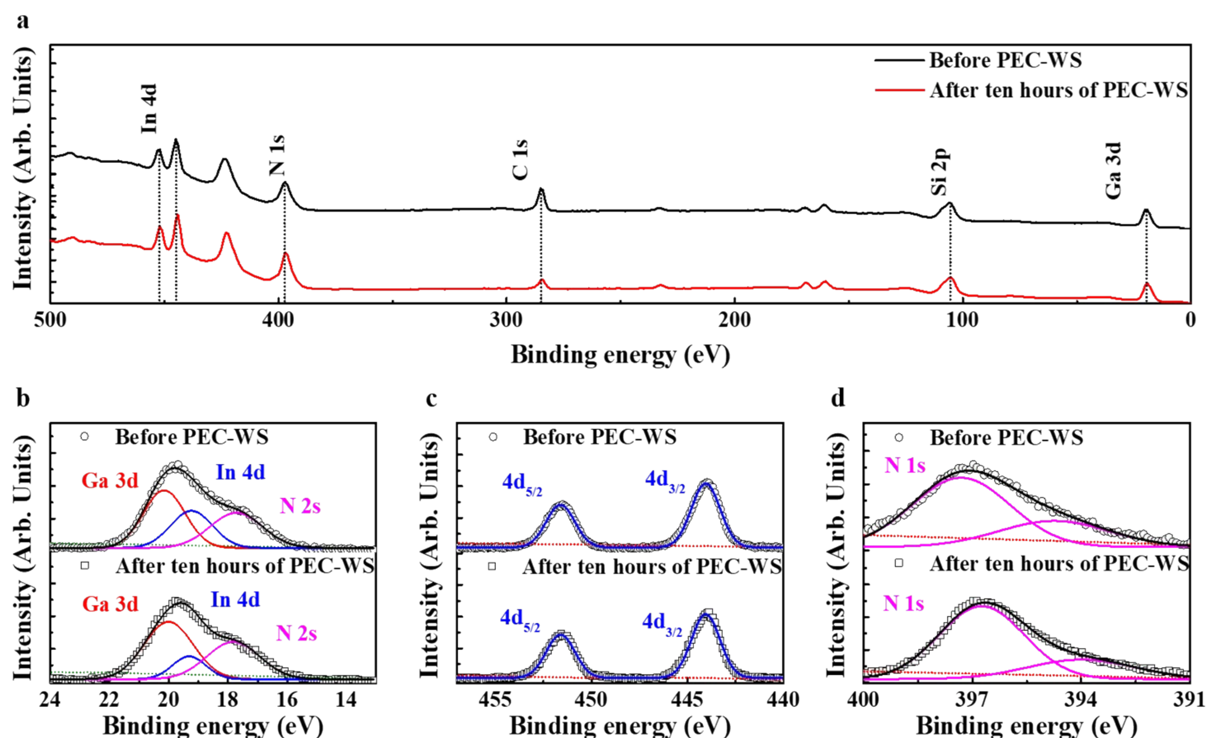

Fig. S7. (a) XPS curves of InGaN/GaN-CSNW PC measured before PEC-WS and after ten hours of the PEC-WS reaction. The XPS curves of the InGaN/GaN-CSNW PC are expanded for the analysis of (b) Ga 3d, (c) In 4d, and (d) N 1s.

PEC-WS performance of InGaN/GaN-CSNW PC with the reproducibility and long-term stability

Fig. S8a shows the time-dependent current density of the InGaN/GaN-CSNW PC measured at a voltage of -1 V versus RHE under illumination for 24 hours. The current density of the InGaN/GaN-CSNW PC increases as the reaction time increases, and reaches 113.24 mA/cm^2 after seven hours of the PEC-WS reaction, which is equivalent to 454.7% of that measured immediately after the reaction started. The amount of hydrogen gas generated by the InGaN/GaN-CSNW PC, calculated from the current density, reached a maximum of 50.53 mmol/cm^2 after operating the PEC-WS reaction for 24 hours. Fig. S8b and c show the OCP and ABPE curves of the InGaN/GaN-CSNW PC measured after 24 hours of PEC-WS, where the performance does not degrade at all compared to that immediately after the reaction.

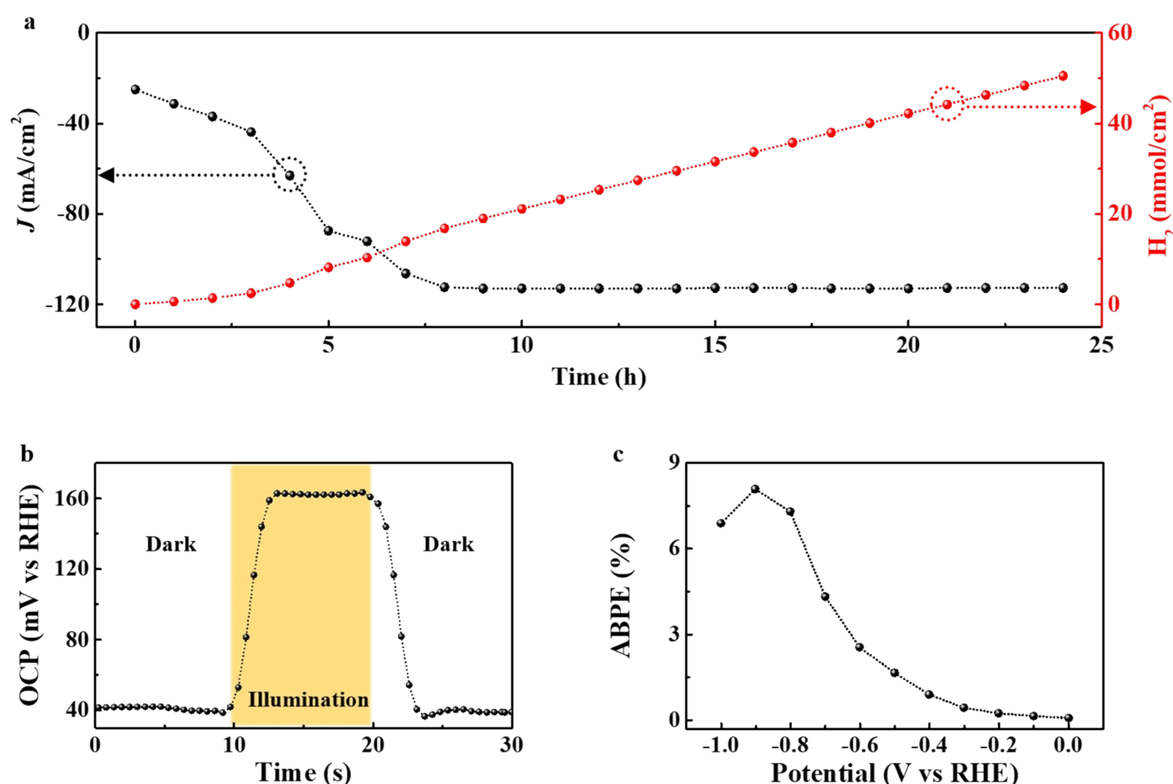

Fig. S8. (a) Time-dependent PEC-WS performance of InGaN/GaN-CSNW PC for 24 hours at a potential of -1 V versus RHE under illumination. (b) OCP and (c) ABPE curves for the InGaN/GaN-CSNW PC of the PEC-WS reaction measured after 24 hours.

Schematic of the offset parameters of an InGaN/GaN CSNW

Fig. S9 schematically shows the offset parameters of an InGaN/GaN core-shell structure.

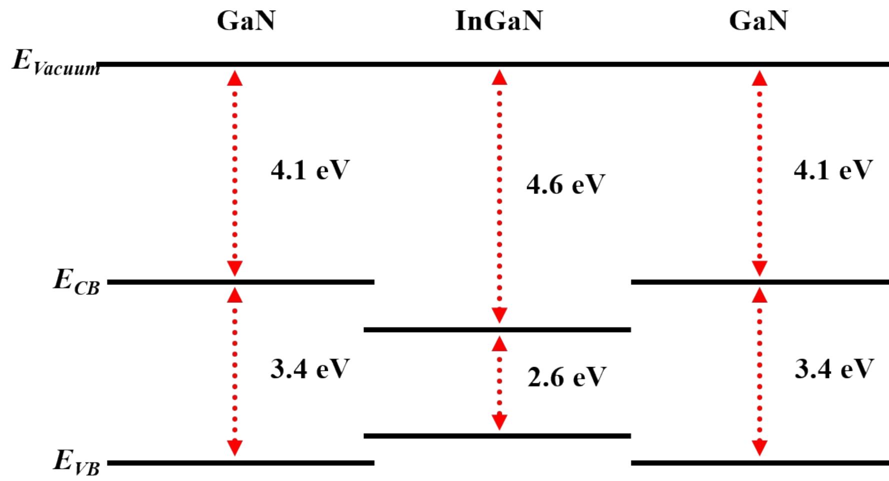

Fig. S9. Schematic of offset parameters for the hetero-interface of an InGaN/GaN CSNW structure.

Supplementary Note S1: Calculation of ABPE

In the PEC-WS system with the three-electrode configuration, an ABPE curve is used to evaluate the performance for solar-water half reaction, i.e., *so-called* hydrogen reduction reaction. For the GaN-NW PA and InGaN/GaN-CSNW PC shown in Fig. 2d, the ABPE values can be calculated using the following equation (1).[15]

$$ABPE\ (\%) = \frac{J(mA/cm^2) \times (1.23 - |V_{app}|)(V\ vs.\ RHE)}{P_{in}(mW/cm^2)} \times 100\% \tag{1}$$

where J is the measured current density, V_{app} represents the external electric bias, and P_{in} is power density of the incident light.

Supplementary Note S2: Calculation of H_2 gas production

Hydrogen gas production from PEC-WS using the InGaN/GaN-CSNW PC in three-electrode configuration for ten hours can be calculated using the following equation (2).[16]

$$Hydrogen\ gas\ production = \frac{\frac{J(A/cm^2) \times t(s)}{e} / 2}{N_A} \tag{2}$$

where J is the measured current density, t is the measurement time, e is the charge of an electron, and N_A is the Avogadro constant.

References

1. I. Choi, H. Lee, C.-R. Lee, K.-U. Jeong and J. S. Kim, Formation of spherical-shaped GaN and InN quantum dots on curved SiN/Si surface. *Nanotechnology* 2018, ***29***, 315603.
2. S. Noh, S. Han, I. Choi, J. S. Kim and M.-Y. Ryu, Formation mechanism of GaN nanowires with various shapes on Si(111). *J. Korean Phys. Soc.* 2020, *77*, 247-252.
3. S. Han, S.-K. Lee, I. Choi, J. Song, C.-R. Lee, K. Kim, M.-Y. Ryu, K.-U. Jeong and J. S. Kim, Highly efficient and flexible photosensors with GaN nanowires horizontally embedded in a graphene sandwich channel. *ACS Appl. Mater. Interfaces* 2018, ***10***, 38173-38182.
4. S. Han, I. Choi, C.-R. Lee, K.-U. Jeong, S.-K. Lee and J. S. Kim, Fast response characteristics of flexible ultraviolet photosensors with GaN nanowires and graphene. *ACS Appl. Mater. Interfaces* 2019, ***12***, 970-979.
5. G. Avit, K. Lekhal, Y. André, C. Bougerol, F. Réveret, J. Leymarie, E. Gil, G. Monier, D. Castelluci and A. Trassoudaine, Ultralong and defect-free GaN nanowires grown by the HVPE process. *Nano Lett.* 2014, ***14***, 559-562.
6. G. Tourbot, C. Bougerol, A. Grenier, M. D. Hertog, D. Sam-Giao, D. Cooper, P. Gilet, B. Gayral and B. Daudin, Structural and optical properties of InGaN/GaN nanowire heterostructures grown by PA-MBE. *Nanotechnology* 2011, ***22***, 075601.
7. A. Wei, X. Xie, Z. Wen, H. Zheng, H. Lan, H. Shao, X. Sun, J. Zhong and S.-T. Lee, Triboelectric nanogenerator driven self-powered photoelectrochemical water splitting based on hematite photoanodes. *ACS Nano* 2018, ***12***, 8625-8632.
8. G. Santana, O. D. De Melo, J. Aguilar-Hernández, R. Mendoza-Pérez, B. M. Monroy, A. Escamilla-Esquivel, M. López-López, F. M. Moure, L. A. Hernández and G. Contreras-Puente, Photoluminescence study of gallium nitride thin films obtained by infrared close space vapor transport. *Materials* 2013, ***6***, 1050-1060.
9. V. P. Kladko, A. V. Kuchuk, H. V. Stanchu, N. V. Safriuk, A. E. Belyaev, A. Wierzbicka, M. Sobanska, K. Klosek and Z. R. Zytkiewicz, Modelling of x-ray diffraction curves for GaN nanowires on Si(111). *J. Cryst. Growth* 2014, ***401***, 347-350.
10. S. Eftychis, J. E. Kruse, K. Tsagaraki, T. Koukoula, T. Kehagias, P. Komninou and A. Georgakilas, Effects of ultrathin AlN prelayers on the spontaneous growth of GaN nanowires by plasma assisted molecular beam epitaxy. *J. Cryst. Growth* 2019, ***514***, 89-97.
11. C. H. Wu, P. Y. Lee, K. Y. Chen, Y. T. Tseng, Y. L. Wang and K. Y. Cheng, Selective area growth of high-density GaN nanowire arrays on Si (111) using thin AlN seeding layers. *J. Cryst. Growth* 2016, ***454***, 71-81.
12. L. W. Tu, C. L. Hsiao, T. W. Chi, I. Lo and K. Y. Hsieh, Self-assembled vertical GaN nanorods grown by molecular-beam epitaxy. *Appl. Phys. Lett.* 2003, ***82***, 1601-1603.
13. Y.-H Ra, R. Navamathavan, J.-H. Park and C.-R. Lee, Coaxial $In_xGa_{1-x}N$/GaN multiple quantum well nanowire arrays on Si (111) substrate for high-performance light-emitting diodes. *Nano lett.* 2013, ***13***, 3506-3516.
14. F. Glas and B. Daudin, Stress-driven island growth on top of nanowires. *Phys. Rev. B* 2012, ***86***, 174112.
15. S. S. Patil, M. A. Johar, M. A. Hassan, D. R. Patil and S.-W. Ryu, Anchoring MWCNTs to 3D honeycomb ZnO/GaN heterostructures to enhancing photoelectrochemical water oxidation. *Appl. Catal. B-Environ.* 2018, ***237***, 791-801.
16. C. Jiang, S. J. A. Moniz, A. Wang, T. Zhang and J. Tang, Photoelectrochemical devices for solar water splitting-materials and challenges. *Chem. Soc. Rev.* 2017, ***46***, 4645-4660.